JOURNAL OF MATERIALS SCIENCE 27 (1992) 1457–1463

Fracture statistic of torsion and flexure in glass rectangular bars

V. MARTINEZ, P. KITTL, G. DIAZ
Departamento de Ciencia e Ingeniería de Materiales, IDIEM, Facultad de Ciencias Físicas y Matemáticas, Universidad de Chile, Casilla 1420, Santiago, Chile

Fracture statistics in rectangular bars subjected to torsion and to three-point bending are studied and the cumulative probabilities of fracture using Weibull's functions for materials that exhibit volume brittleness are determined. Diagrams of the cumulative probability fracture for commercial glass samples are plotted. The parameters of Weibull's functions regarding torsion and bending are appraised by employing lineal regression and nomograms, respectively. For torsion, dispersion of the parameters is determined by resorting to Fisher's information matrix. The size effect experimentally determined becomes half of the same theoretically determined. The different forms of the statistical functions followed by the same material in the two tests, are due to form and size influences of the cracks originating at the fracture, as well as to the finish of the sample sides.

1. Introduction

The probabilistic strength of bars subjected to torsion was theoretically and experimentally studied by Díaz and Morales [1] in the case of round bars. In this work a comparison of the experimental results of fracture statistics of torsion and flexure in glass cylinders was studied and parameters for the Weibull and Kies–Kittl functions were obtained using the nomogram method. More recently the case of a prismatic bar subjected to torsion whose cross-section is a regular polygon was treated by Díaz and Kittl [2]. The square bar was studied by Díaz and Kittl [3] and an elliptical bar by Kittl *et al.* [4] from a theoretical viewpoint. A probabilistic approach to the case of cylinders subjected to torsion has been discussed [5–9].

The aim of this work is an experimental study of the probabilistic strength of a rectangular bar subjected to pure torsion and bending using the stress field obtained through elasticity theory and applied to commercial glass samples. The nomogram method is used to obtain the Weibull parameters and dispersion of the same is determined resorting to Fisher's information matrix.

2. Statistic of fracture through torsion

The cumulative probability of fracture $F(\tau)$ for materials exhibiting volume brittleness and subjected to some uniaxial state of shear stress is as follows according to Weibull's theory

$$F(\tau) = 1 - \exp\left(-\frac{1}{V_0}\int_V \phi[\tau(r)]\,dV\right) \quad (1)$$

where V_0 is the volume unit, V the body volume, r the position vector, τ the maximum shear stress reached in the material before breaking, $\tau(r) \leqslant \tau$ the stress field, and $\phi(\tau)$ the specific risk-of-fracture function. Weibull [10] has proposed the following analytical form for this function:

$$\phi(\tau) = \begin{cases} \left(\dfrac{\tau - \tau_L}{\tau_0}\right)^m & \tau \geqslant \tau_L \\ 0 & \tau < \tau_L \end{cases} \quad (2)$$

where τ_0 and m are the parameters depending on the manufacturing process of the material, while τ_L is the stress under which there is no fracture.

Consider a bar of length L with a rectangular cross-section with half minor side a and half major side b and let us assume that bar is not subjected to any internal force, and is free from external lateral forces. One end of the bar is fixed on to the plane $x = 0$ while the other end located in the plane $x = L$, is twisted by a couple of magnitude M whose moment is directed along the bar axis. The rectangular coordinates' origin is located at the gravity centre of the fixed base, the x axis coinciding with the directrix while the y and z axes are the principal axes of inertia of the section. The stresses are obtained from the elasticity theory [11], as follows:

$$\tau_{XY} = \frac{9M}{16ab^3} z\left(1 - \frac{y^2}{a^2}\right)$$
$$\tau_{XZ} = -\frac{9M}{16a^3b} y\left(1 - \frac{z^2}{b^2}\right) \quad (3)$$

therefore the stress field in a rectangular bar is given by

$$\tau(y, z) = (\tau_{xz}^2 + \tau_{xy}^2)^{1/2}$$
$$= \frac{\tau}{ab^2}[z^2(a^2 - y^2)^2 + y^2(b^2 - z^2)^2]^{1/2}$$
$$\leqslant \tau = \frac{9M}{16a^2b}$$
$$0 \leqslant y \leqslant a, \quad 0 \leqslant z \leqslant b, \quad 0 \leqslant x \leqslant L \quad (4)$$

0022–2461

using the following change of variables

$$\eta = \frac{y}{a}; \quad \zeta = \frac{z}{b} \tag{5}$$

$$\xi(\tau) = \frac{2Lab}{V_0(m+1)}\left(\frac{\tau_L}{\tau_0}\right)^m \frac{1}{\tau/\tau_L}\int_1^{\tau/\tau_L} \frac{(\eta-1)^{m+1}}{\eta[1-(\tau_L/\tau)\eta]^{1/2}}\,d\eta \qquad e = 0 \tag{12}$$

$$\xi(\tau) = \frac{4La^2}{V_0}\left(\frac{\tau_L}{\tau_0}\right)^m I_2\left(1, m, \frac{\tau}{\tau_L}\right) \qquad e = 1 \tag{13}$$

then, the stress field defined in Equation 4 becomes

$$\tau(\eta,\zeta) = \tau[e^2\zeta^2(1-\eta^2)^2 + \eta^2(1-\zeta^2)^2]^{1/2}$$
$$\leqslant \tau = \frac{9M}{16a^2b} \tag{6}$$
$$0 \leqslant \eta \leqslant 1, \quad 0 \leqslant \zeta \leqslant 1, \quad 0 \leqslant x \leqslant L, \quad e = a/b.$$

Two particular instances are of special interest, namely the cases wherein $e = 0$ and $e = 1$. The first case corresponds to the stress field of a thin rectangular bar wherein the ratio $a/b = e$ tends towards zero, while the second case represents the stress field in a square bar.

Equation 1 can be rewritten as follows:

$$\xi(\tau) = \ln\frac{1}{1-F(\tau)} = \frac{1}{V_0}\int_V \phi[\tau(r)]\,dV \tag{7}$$

where $\xi(\tau)$ is the Evans' function [12].

If $\phi(\tau)$ is given by Equation 2 with $\tau_L = 0$, i.e. using the defined functions method, and considering the above Equations 5, 6 and 7 we obtain [13]

$$\left.\begin{aligned} \xi(\tau) &= \frac{4Lab}{V_0}\left(\frac{\tau}{\tau_0}\right)^m I_1(e,m) \\ I_1(e,m) &= \int_0^1\int_0^1 [e^2\zeta^2(1-\eta^2)^2 + \eta^2(1-\zeta^2)^2]^{m/2}\,d\eta\,d\zeta \end{aligned}\right\} \quad e \in [0,1] \tag{8}$$

and considering the limit cases of a thin rectangular bar and a square bar, above Equation 8 becomes

$$\xi(\tau) = \frac{2(\pi)^{1/2}Lab}{V_0(m+1)}\frac{\Gamma(m+1)}{\Gamma(m+\frac{3}{2})}\left(\frac{\tau}{\tau_0}\right)^m \qquad e = 0 \tag{9}$$

$$\xi(\tau) = \frac{4La^2}{V_0} I_1(1,m)\left(\frac{\tau}{\tau_0}\right)^m \qquad e = 1 \tag{10}$$

wherein $\Gamma(m)$ is the Euler gamma function.

On the other hand, if the specific risk-of-fracture function $\phi(\tau)$ is expressed by means of Equation 2 with $\tau_L \neq 0$, then the consideration of Equations 5, 6 and 7 yields [13]

$$e \in [0,1] \quad \left\{\begin{aligned} \xi(\tau) &= \frac{4Lab}{V_0}\left(\frac{\tau_L}{\tau_0}\right)^m I_2\left(e, m, \frac{\tau}{\tau_L}\right) \\ I_2\left(e, m, \frac{\tau}{\tau_L}\right) &= \iint_{\mathscr{R}}\left(\frac{\tau}{\tau_L}[e^2\zeta^2(1-\eta^2)^2 + \eta^2(1-\zeta^2)^2]^{1/2} - 1\right)^m d\eta\,d\zeta \\ \mathscr{R} &= \left\{(\eta,\zeta)/e^2\zeta^2(1-\eta^2)^2 + \eta^2(1-\zeta^2)^2 \geqslant \left(\frac{\tau_L}{\tau}\right)^2;\ 0 \leqslant \eta \leqslant 1; 0 \leqslant \zeta \leqslant 1\right\} \end{aligned}\right. \tag{11}$$

and considering the limit cases of a thin rectangular bar and a square bar, above Equation 11 becomes [13]

If some known analytical form is not assumed for $\phi(\tau)$, i.e. using the integral equations method [14], then Equations 5, 6 and 7 allow us to obtain the following integral equation [13]:

$$\xi(\tau) = \frac{4Lab}{V_0}\int_0^1\int_0^1 \phi\{\tau[e^2\zeta^2(1-\eta^2)^2 + \eta^2(1-\zeta^2)^2]^{1/2}\}\,d\eta\,d\zeta \tag{14}$$

whose solution is obtained by means of Taylor series expansions as follows [13]:

$$\phi(\tau) = \frac{V_0}{4Lab}\sum_{n=0}^{\infty}\frac{\xi^{(n)}(0)}{n!I_1(e,n)}\tau^n \qquad e \in [0,1] \tag{15}$$

and considering the limit cases of a thin rectangular bar and the square bar, above Equation 15 becomes [13]

$$\phi(\tau) = \frac{V_0}{2(\pi)^{1/2}Lab}\sum_{n=0}^{\infty}\frac{(n+1)\Gamma(n+\frac{3}{2})\xi^{(n)}(0)}{n!\Gamma(n+1)}\tau^n \qquad e = 0 \tag{16}$$

$$\phi(\tau) = \frac{V_0}{4La^2}\sum_{n=0}^{\infty}\frac{\xi^{(n)}(0)}{n!I_1(1,n)}\tau^n \qquad e = 1 \tag{17}$$

Furthermore, in the particular case of a thin rectangular bar when $e = 0$, the integral equation can be solved using a finite integral–differential operator. The integral equation is transformed into an Abelian integral equation whose solution yields [13]

$$\phi(\tau) = \frac{V_0}{2\pi Lab}\frac{d}{d\tau}\left(\tau\int_0^{\tau}\frac{d}{d\eta}[(\eta)^{1/2}\xi(\eta)]\frac{d\eta}{(\tau-\eta)^{1/2}}\right) \tag{18}$$

3. Statistic of fracture through flexure

For the case of a rectangular bar subjected to three-point bending, the cumulative probability of fracture

is theoretically known for all cases of brittleness [15]. In this work, we take only results of the defined functions method in volume brittleness. So then, the Evans' function [12] when $\phi(\tau)$ is a Weibull's function with $\sigma_L = 0$, is

$$\xi(\sigma) = \ln\frac{1}{1 - F(\sigma)} = \frac{bhL}{2(m + 1)^2 V_0}\left(\frac{\sigma}{\sigma_0}\right)^m \tag{19}$$

and considering that $\phi(\sigma)$ is a Weibull's function with $\sigma_L \neq 0$

$$\xi(\sigma) = \ln\frac{1}{1 - F(\sigma)} = \frac{bhL}{2V_0(m + 1)}\left(\frac{\sigma_L}{\sigma_0}\right)^m \frac{1}{\sigma/\sigma_L} \times \int_1^{\sigma/\sigma_L} \frac{(\eta - 1)^{m+1}}{\eta} d\eta \tag{20}$$

4. Parameter estimation

For estimating parameters in flexure or torsion, it is convenient to use a graphical method which consists of obtaining the mentioned parameters by comparison using a non-dimensional nomogram [16–20].

The general expression of the cumulative probability of fracture function can be rewritten as follows, when the specific risk-of-fracture function is given by Equation 2

$$F(\sigma) = 1 - \exp\left[-g\left(\frac{V}{V_0}, m\right)\left(\frac{\sigma_L}{\sigma_0}\right)^m \xi'\left(\frac{\sigma}{\sigma_L}, m\right)\right] \tag{21}$$

where g is a non-dimensional function of material geometry and of parameter m. Rearranging Equation 21 and taking into account Equation 7 we obtain

$$\ln\xi(\sigma) = \ln\xi'\left(\frac{\sigma}{\sigma_L}, m\right) + \ln\left[g\left(\frac{V}{V_0}, m\right)\left(\frac{\sigma_L}{\sigma_0}\right)^m\right] \tag{22}$$

$$C = \ln\left[g\left(\frac{V}{V_0}, m\right)\left(\frac{\sigma_L}{\sigma_0}\right)^m\right] \tag{23}$$

Now, plotting $\ln\xi'(\sigma/\sigma_L, m)$ against $\ln(\sigma/\sigma_L)$ for diverse values of Weibull's parameters m supplies a non-dimensional graph called a nomogram.

The parameters m, σ_0 and σ_L for a particular case are obtained by drawing a Weibull diagram on transparent paper using therefore the experimental points; in other words, $\ln\xi(\sigma)$ is plotted against $\ln\sigma$ and then moved parallel to $\ln\xi'$ and $\ln(\sigma/\sigma_L)$ axes so that the experimental points are fitted to some corresponding nomogram curve. This provides the immediate determination of the parameter m. Then the coordinates of the origin of the system $\ln\xi'$ plotted against $\ln(\sigma/\sigma_L)$, with respect to the system $\ln\xi(\sigma)$ plotted against $\ln\sigma$ allow the other two parameters to be determined. The coordinates of the nomogram origin are $(C, \ln\sigma_L)$. The value of constant C is measured by the vertical distance between the horizontal axis of the nomogram and the horizontal axis of the plotting of the experimental points. Equation 23 is used to obtain parameter σ_0.

When the specific risk-of-fracture function is given by Equation 2 with $\sigma_L = 0$, then a Weibull's diagram can be plotted and parameters are obtained from the respective lineal regression.

In three-point bending, nomograms were derived by León and Kittl [20] using the following expressions for ξ' and C:

$$\xi' = \frac{m + 1}{(\sigma/\sigma_L)^m}\int_1^{\sigma/\sigma_L} \frac{(\eta - 1)^{m+1}}{\eta} d\eta$$
$$C = \ln\frac{bhL}{2V_0(m + 1)^2}\left(\frac{\sigma_L}{\sigma_0}\right)^m \tag{24}$$

In torsion of a rectangular bar, nomograms were derived for the present work using the following expressions for ξ' and C:

$$\xi' = I_2\left(e, m, \frac{\tau}{\tau_L}\right)$$
$$C = \ln\left[\frac{4Lab}{V_0}\left(\frac{\tau_L}{\tau_0}\right)^m\right] \tag{25}$$

The first case required plotting $\ln\xi'$ against $\ln(\sigma/\sigma_L)$ for diverse values of Weibull's parameter m. In the torsion case, plotting $\ln\xi'$ against $\ln(\tau/\tau_L)$ for diverse values of Weibull's parameter m was required and, in addition, for diverse values of geometrical parameter $e = a/b$. We, therefore, obtain a set of nomograms for values of e between $e = 0$ and $e = 1$.

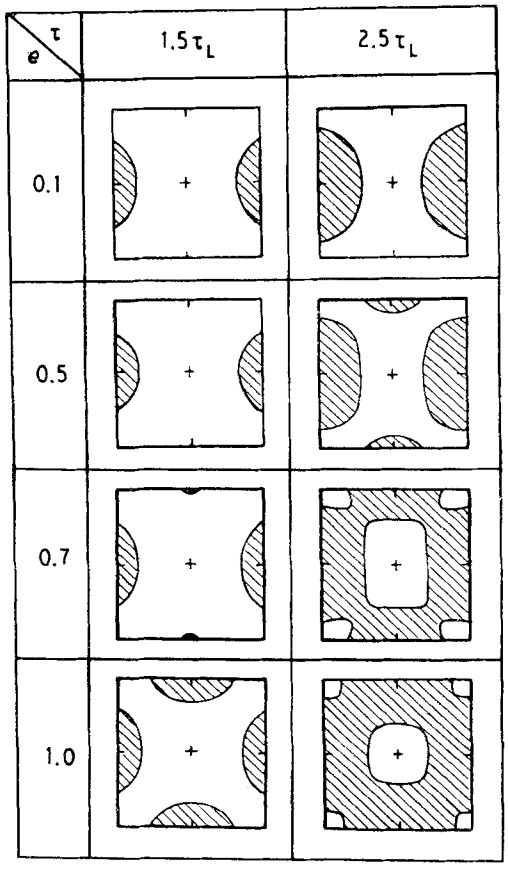

Figure 1 Non-dimensional diagrams. The hatched regions are the zones to the integration dominion $\mathscr{R}$ in Equation 11.

On the other hand, in the torsion case it is possible to obtain diagrams which show the zones on the cross-section wherein Equation 11 is defined. This was obtained by numerical methods putting $\xi(\tau) = 0$ in Equation (11) and entering values for parameter e and the ratio τ_L/τ. Fig. 1 shows non-dimensional diagrams for the rectangular cross-section showing those zones (which is transformed into a square cross-section with sides equal to 2). The hatched regions correspond to the regions wherein $\tau/\tau_L > 1$ and they are the zones corresponding to the integration dominion $\mathscr{R}$ in Equation 11.

5. Experimental procedure

230 samples of commercial glass 0.0024 m in height and 0.015 m in width were used, 48 samples 0.089 m in length and 50 samples 0.040 m in length were subjected to a fracture test through flexure, and 91 samples 0.10 m in length and 41 samples 0.05 m in length were subjected to a fracture test through torsion. The torsion arrangement included a loading disc $R = 0.07$ m in radius, a balance and a receptacle hanging on the disc, and this arrangement was mounted on a machine tool lathe. Specimen holders made of steel were constituted by a mechanical system of screws with double screw thread designed specially for holding the samples. This arrangement allowed us to axially insert one of the specimen holders in a tailstock's centre sleeve of the lathe while the other specimen holder was inserted in axial fashion in the loading disc, thus avoiding damage to the specimens during the test. The load Q of fracture through torsion was applied by introducing a number of small weights in the said loading receptacle. Upon specimen fracturing these weights were totalled in order to ascertain Q. The maximum stress of torsional fracture is then given by

$$\tau = \frac{9QR}{16a^2b} \tag{26}$$

wherein a is equal to half height and b is equal to half width and they correspond to the half of the sides of the rectangular cross-section.

The flexure test was a three-point bending test where the load P was concentrated at the centre of the sample. For this purpose a box of steel was constructed with supports and a system for applying the load through the introduction of small weights in a receptacle. The balance was used to measure the load P. The maximum stress of flexural fracture is given by

$$\sigma = \frac{3}{2}\frac{PL}{bh^2} \tag{27}$$

where h is equal to the height, b the width and L the length of the sample.

The experimental results were plotted in a diagram of the cumulative probability of fracture, for both lengths in each one of the considered tests. The said probability was determined using

$$F(\sigma) = \frac{i - \frac{1}{2}}{N} \tag{28}$$

where $F(\sigma)$ is the cumulative probability of fracture, i the number of samples that failed under some stress at most equal to σ, and N the number of the samples tested.

6. Analysis of the results and discussion

Fig. 2 shows the cumulative probability of fracture for samples tested through torsion with length equal to 0.10 m and through flexure with length equal to 0.089 m. First, let us consider the curve corresponding to torsion, located at the right-hand side in the graph. The experimental data were distributed in accordance with a Weibull's specific risk-of-fracture function of two parameters, that is to say, a function given by Equation 2 with $\tau_L = 0$. Second, the curve shown at the left-hand on Fig. 2 corresponds to the experimental data supplied by the three-point bending test. We can see that these data followed a distribution in keeping with a Weibull's function of three parameters given by Equation 2 with $\sigma_L \neq 0$. Fig. 3 is analogous to Fig. 2 for samples 0.040 m long in torsion and for samples 0.050 m long in flexure. This fact, namely the different fracture statistics followed by the same material in the torsional and flexural tests may be explained as follows. In torsion, fracturing is strongly by shear and because the samples were obtained by cutting from a commercial glass, hence the form and size of the resultant cracks on the lateral edges appear to have a great influence on this process and then the maximum stress does not have either an upper limit or a lower limit. On the other hand, in flexure, fracturing is through traction and the form and size of the cracks coming from the manufacturing process are very important and because the sides subjected to traction have a good finish and, in consequence, small cracks, the maximum stress has a very large upper boundary and a lower limit σ_L. The reason for the difference in fracture statistics between torsion and flexure may not be due to the fact that the torsion or the flexure experimental configuration would introduce another

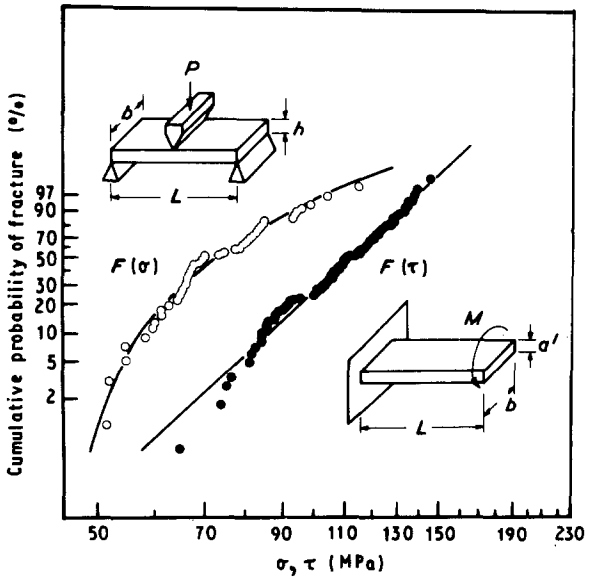

Figure 2 Long specimens subjected to flexure (○) and torsion (●). $a' = 2a$, $b' = 2b$.

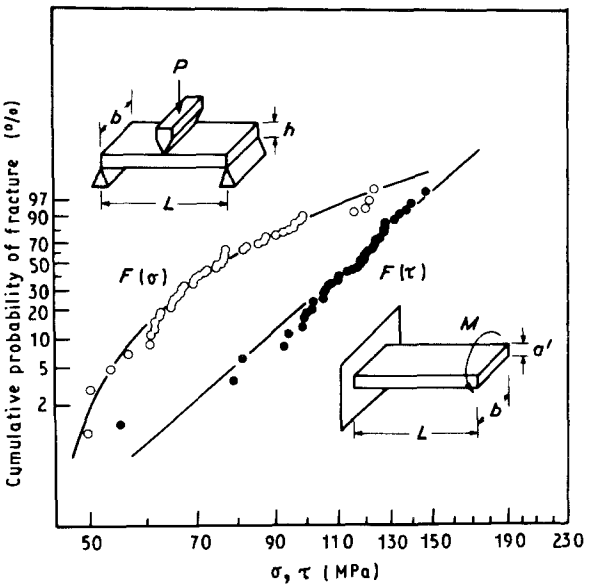

Figure 3 Short specimens subjected to flexure (○) and torsion (●). $a' = 2a$, $b' = 2b$.

stress than that shown herein. If so in torsion, these stresses would be flexure stresses and in the event of becoming large then the experimental curve of torsion should exhibit some shape similar to that of the experimental curve of flexure, excepting a certain shifting due to size effect. Experimental findings show, however, that such an introduction of flexure stresses is null or negligible.

The parameters of the Weibull function of the specific risk-of-fracture with $\tau_L = 0$, in the torsion case, were evaluated through a lineal regression. Rearranging Equation 8 gives

$$\ln \xi(\tau) = m \ln \tau + \ln \frac{4Lab}{V_0 \tau_0^m} I_1(e, m). \quad (29)$$

Establishing a comparison between the lineal regression applied to the experimental points and Equation 29, the values of the parameters are, therefore, determined in a direct form. The parameters of the Weibull function of the specific risk-of-fracture with $\sigma_L \neq 0$, in the flexure case, were evaluated by preparing a non-dimensional nomogram. Fig. 4 shows how the value of the constant C is graphically ascertained by measuring the vertical distance between the horizontal axis of the distribution of the nomogram and the horizontal axis of the experimental points.

The minimum chi-square was used as an estimator for the adjustment between the probability distribution used and the data in both tests. It is a squared error-consistent estimator under quite general conditions and is given by

$$\chi^2 = \sum_{i=1}^{r} \frac{(K_i - tF_i)^2}{tF_i}; \qquad \sum_{i=1}^{i=r} K_i = t \quad (30)$$

where the population is classified into r classes each comprising k_i elements, t is the number of trials and F_i the probability of failure in the classes.

The dispersion of the parameters of the cumulative probability-of-fracture functions may be estimated through Fisher's information matrix [21]. The coefficients of the Fisher matrix are determined using

$$r_{ij} = -n \int \left(\frac{\partial^2 \ln f(\tau; \theta)}{\partial \theta_i \partial \theta_j} \right) f(\tau) \, d\tau \quad (31)$$

where r_{ij} is the coefficient i, j; n the sample size, θ the parameters, and $f(\tau) = dF(\tau)/d\tau$ the density function of fracture probability. The simple structure of the function of the cumulative probability of torsional fracture, when the specific risk-of-fracture function is a Weibull function with $\tau_L = 0$, renders if possible to resort to the Fisher's matrix. In this case, the elements of the matrix become

$$\begin{aligned} r_{11} &= n\left(\frac{1}{K}\frac{\partial K}{\partial m}\right)^2 + \frac{2n}{Km}\frac{\partial K}{\partial m}(0.42277 - \ln K) \\ &\quad + \frac{n}{m^2}(1.82379 - 0.84555 \ln K + \ln^2 K) \\ r_{12} &= -\frac{n}{\tau_0}\left(\frac{m}{K}\frac{\partial K}{\partial m} - \ln K + 0.42277\right) \quad (32) \\ r_{22} &= n\left(\frac{m}{\tau_0}\right)^2 \end{aligned}$$

where

$$K = \frac{4Lab}{V_0} I_1(e, m)$$

When $\tau_L = 0$, the matrix of variances and covariances is easily obtained through the inversion of the Fisher matrix, with the condition that $r_{11} \geqslant 0$. So then, variances and covariances were determined using

$$\begin{aligned} \mathrm{var}(m) &= \frac{r_{22}}{r_{11}r_{22} - r_{12}^2} \\ \mathrm{var}(\tau_0) &= \frac{r_{11}}{r_{11}r_{22} - r_{12}^2} \quad (33) \\ \mathrm{cov}(m, \tau_0) &= \frac{r_{12}}{r_{12}^2 - r_{11}r_{22}} \end{aligned}$$

In the flexure case where $\sigma_L \neq 0$, the required calculation in the Fisher matrix is very cumbersome, and hence it becomes more convenient to use another method to obtain the dispersion of the parameters; for instance, the Monte-Carlo simulation method may be resorted to.

The values of the parameters were indicated in Tables I and II, along with the mean stress fracture and the χ^2 of the distribution of probability used, for both lengths in each one of the two tests. In addition, the variances of the parameters are indicated for the torsion case.

The size effect [22] was studied for both tests. The experimental points of the two tests of torsion for both lengths were plotted in on one graph. The same was done for the flexure tests. The graphs show a separation between the distributions, that could correspond to the size effect. To ascertain this fact, it is necessary to establish a comparison between what is expected by the theory and what is found by experiment. Let us then take Equation 8 rewritten for two volumes given by $L = 0.10$ m (long specimens) and $L = 0.05$ m (short

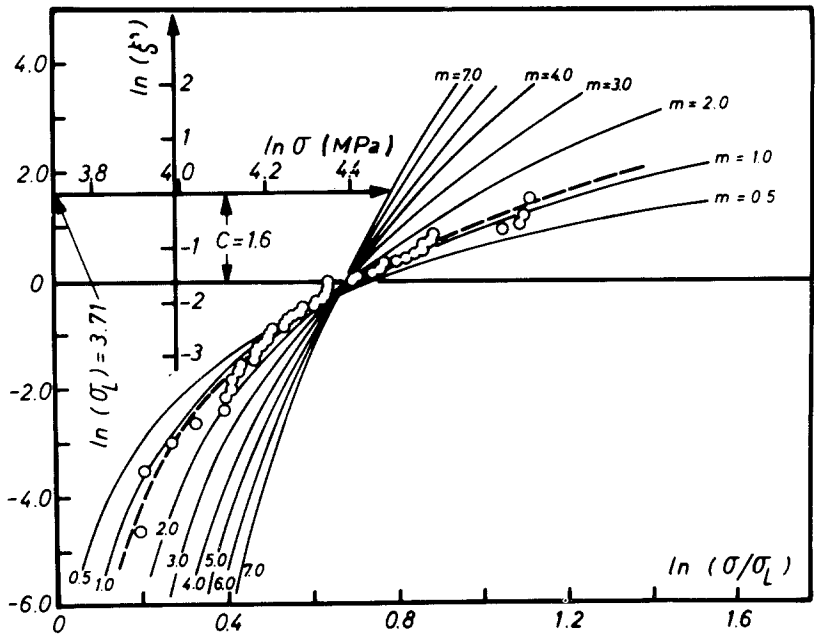

Figure 4 Weibull's function nomogram used to obtain the Weibull's parameters in the flexure test. (○) Long specimens.

TABLE I Weibull's parameters, mean strength, variances and chi-square estimator for both lengths used in the torsion test. j = class number

Torsion test		Short specimens $L = 0.040$ m	Long specimens $L = 0.089$ m
	m	7.091	7.512
Parameters	τ_0 (MPa)	11.87	14.09
Mean strength	τ (MPa)	113.56	109.22
Variances	Var (m)	0.17	0.38
	Var (τ_0)	1.42	4.41
Chi-square	χ^2	7.97 ($j = 9$)	4.71 ($j = 8$)
	$\chi^2_{0.95\,(j=3)}$	12.6	11.1

TABLE II Weibull's parameters, mean strength and chi-square estimator for both lengths used in the flexure test. j = class number

Flexure test		Short specimens $L = 0.05$ m	Long specimens $L = 0.10$ m
	m	1.2	1.2
Parameters	σ_0 (MPa)	2.2×10^{-5}	2.7×10^{-5}
	σ_L (MPa)	40.85	42.52
Mean strength	σ (MPa)	78.35	73.80
Chi-square	χ^2	10.0 ($j = 10$)	7.81 ($j = 8$)
	$\chi^2_{0.95\,(j=4)}$	12.6	9.49

specimens) in the torsion case

$$\ln \xi_L(\tau) = \ln\left(\frac{V_L}{V_0}\right) + \ln\left(\frac{\tau}{\tau_{0L}}\right)^{m_L} I_1(e_L, m_L) \quad (34)$$

$$\ln \xi_S(\tau) = \ln\left(\frac{V_S}{V_0}\right) + \ln\left(\frac{\tau}{\tau_{0S}}\right)^{m_S} I_1(e_S, m_S) \quad (35)$$

where the subscript L indicates the long specimens and subscript S the short specimens. Substracting Equation 34 from Equation 35 and assuming that parameters are the same for both volumes, and

TABLE III Size effect in torsion and flexure tests

		Torsion	Flexure
Theoretical result			
Second member of Equation 36		0.685	0.792
	Long specimens	0.2739	0.378
Experimental result			
First member of Equation 36	Short specimens	0.2900	0.398

$e_L = e_S$, gives

$$\ln \xi_L(\tau) - \ln \xi_S(\tau) = \ln\left(\frac{V_L}{V_S}\right) \quad (36)$$

In order to establish a comparison between two members of Equation 36, we calculate the mean-fracture stress for the two lengths after evaluating the first member of Equation 36 for the two mean-stresses and the second member for the ratio of volumes. The same is done for flexure. The results of the calculations are shown in Table III. It is clear that the experimental size effect is approximately a half that of the theoretical value. This last fact may be due to the existence of random boundary conditions coming from experimental configuration such as axes put off-centre, absence of parallelism and other effects which would be why the shifting is less than that theoretically expected.

7. Conclusions

The problem of obtaining the specific risk-of-fracture function for the cases of torsion and flexure has been completely solved using the defined-functions method. The different fracture statistics followed by the commercial-glass samples when subjected to torsion or to flexure, are due to the influence of the finish of the edges.

In the case of torsion (fracture is strongly by shear), the form and size of the resultant cracks on the lateral edges appear to have a great influence on this process, which involves the existence on neither of upper limit nor of lower limit, and the statistics followed were Weibull statistics with $\tau_L = 0$. On the other hand, in the case of flexure (fracture is through traction), the form and size of the cracks coming from the manufacturing process are very important and because the sides subjected to traction have a good finish, there exists a very large upper boundary and a lower limit σ_L, and the statistics followed were Weibull statistics with $\sigma_L \neq 0$.

In torsion, diagrams for integration dominion of $\xi(\tau)$ have been obtained by numerical methods. It should be emphasized that the integral equation method has a difficult application to the torsion case because the form of the equation involves the existence of a Taylor series expansion, but it is important because, without assuming some known analytical form for the specific risk-of-fracture function, the same may be obtained by applying some numerical method to the function $\xi(\tau)$ which is known from practical experience. When $e = 0$ it, however, corresponds to the case of a thin rectangular bar and the integral equation is transformed into an Abelian integral equation whose solution for $\phi(\tau)$ can be obtained by derivation from Equation 18. The experimental result for the size effect is approximately a half of the theoretical result of the same, for both tests carried out. This last fact can be due to the existence of random boundary conditions.

Acknowledgements

The authors wish to thank the Fondo Nacional de Desarrollo Científico y Tecnológico (FONDECYT) for Grant No 516/88, the Exclusive Dedication Program (1988) of the University of Chile, Professor E. Retamal, Director of the IDIEM Institute for his enthusiastic support concerning the progress of Materials Science, and R. Toledo for his help with the reading of the manuscript.

References

1. G. DIAZ and M. MORALES, *J. Mater. Sci.* **23** (1988) 2444.
2. G. DIAZ and P. KITTL, *Res. Mech.* **29** (1990) 359.
3. G. DIAZ and P. KITTL, *Rev. Mater. Apl.* **10** (1989) 123.
4. P. KITTL, G. DIAZ and V. MARTINEZ, *Res. Mech.* To be published.
5. W. KROENKE, *J Amer. Ceram. Soc.* **49** (1966) 508.
6. J. J. PETROVIC and M. G. STOUT, *ibid.* **64** (1981) 656.
7. J. J. PETROVIC and M. G. STOUT, *ibid.* **64** (1981) 661.
8. M. G. STOUT and J. J. PETROVIC, *ibid.* **67** (1984) 14.
9. J. J. PETROVIC and M. G. STOUT, *ibid.* **67** (1984) 18.
10. W. WEIBULL, *Ing. Vetenskaps Akad. Handl.* **151** (1939) 1.
11. A. FÖPPL, Ed. Gauthier–Villars, Paris (1901) 319–327.
12. A. G. EVANS and R. L. JONES, *J. Amer. Ceram. Soc.* **61** (1978) 156.
13. P. KITTL, G. DIAZ and V. MARTINEZ, To be published.
14. P. KITTL and G. DIAZ, *Res. Mech.* **18** (1986) 207.
15. P. KITTL, *ibid.* **1** (1980) 161.
16. K. TRUSTRUM and A. de S. JAYATILAKA, *J. Mater. Sci.* **14** (1979) 1080.
17. P. KITTL, M. LEON and G. M. CAMILO, Vol. 4, edited by S. R. Valluri, D. M. R. Taplin, P. Ramarao, J. F. Knott and R. Dubey (Pergamon, Oxford, 1985) pp. 2743.
18. M. LEON and P. KITTL, *Latin Am. J. Metall. Mater.* **4** (1984) 103.
19. W. TRADINIK, K. KROMP and R. F. PABST, *Materialprüf* **23** (1981) 42.
20. M. LEON and P. KITTL, *J. Mater. Sci.* **20** (1985) 3778.
21. A. MOOD and F. A. GRAYBILL (McGraw Hill, New York, 1962) pp. 308–311.
22. P. KITTL and G. DIAZ, *Res. Mech.* **24** (1988) 99–207.

Received 11 June 1990
and accepted 31 January 1991